Thalamic Nuclei Volumes Across Psychiatric and Neurological Disorders: A Multi-Site Magnetic Resonance Imaging Study

Running title: Thalamic Nuclei Volumes Across Brain Disorders

***Mäki-Marttunen**, V.[1]*, Nerland, S.[1, 2], Jørgensen, K.[1,3], Høgestøl, E.[4,5,6], Rokicki, J[7], Alnæs, D.[1,6], Borgwardt, S.[8,9], Boye, B.[10,11], Buitelaar, J[12,13], Bøen, E.[10], Cervenka, S.[14,15], Conzelmann, A.[16,17,18], Erhardt, S.[19], Franke, B.[20], Celius, E. G.[4,5], Harbo, H.[4,5], Hilland, E.[21], Hoekstra, P.[22], Hartman, C.A.[23], Jonassen, R.[21], Jönsson, E. G.[1,14], Landrø, N.[2,6], Lesch, K-P.[24,25,26], Maglanoc, L.[27], Pauli, P.[28], Sellgren, C.M.[14,19], Nygaard, G.[4], Oosterlaan, J.[29,30,31], Schmidt, A.[8], Schwarz, E.[19,33], Ziegler, G.C.[24], Agartz, I.[1,2,14], Westlye, L.T.[1,6,34], Andreassen, O.[1,34], Kaufmann, T.[1,18,35], Elvsåshagen, T[1,4,11].*

1. Centre for Precision Psychiatry, Institute of Clinical Medicine, University of Oslo & Division of Mental Health and Addiction, Oslo University Hospital, Oslo, Norway
2. Department of Psychiatric Research, Diakonhjemmet Hospital, Oslo, Norway
3. Division of Mental Health and Addiction, Vestre Viken Hospital Trust, Drammen, Norway
4. Department of Neurology, Division of Clinical Neuroscience, Oslo University Hospital, Oslo, Norway
5. Institute of Clinical Medicine, University of Oslo, Oslo, Norway
6. Department of Psychology, University of Oslo, Oslo, Norway
7. Centre for Research and Education in Forensic Psychiatry (SIFER), Oslo University Hospital, Norway
8. Department of Psychiatry and Psychotherapy, Department of Psychosomatics and Psychotherapy, Centre of Integrative Psychiatry, Schleswig-Holstein University Hospital, Campus Lübeck, Germany
9. Institute of Psychiatry, King's College, London, UK
10. Psychosomatic and CL Psychiatry, Division of Mental Health and Addiction, Oslo University Hospital, Oslo, Norway
11. Department of Behavioural Sciences in Medicine, University of Oslo, Oslo, Norway
12. Department of Cognitive Neuroscience, Donders Institute for Brain, Cognition and Behaviour, Radboud University Medical Center, Nijmegen, The Netherlands
13. Karakter Child and Adolescent Psychiatry University Centre, Nijmegen, The Netherlands
14. Centre for Psychiatry Research, Department of Clinical Neuroscience, Karolinska Institutet & Stockholm Health Care Services, Stockholm Region, Stockholm, Sweden
15. Department of medical sciences, Psychiatry, Uppsala University, Uppsala, Sweden
16. Department of Child and Adolescent Psychiatry, Psychosomatics and Psychotherapy, University Hospital of Psychiatry and Psychotherapy, Tübingen, Germany;
17. DZPG (German Center for Mental Health), partner site Tübingen;
18. PFH – Private University of Applied Sciences, Department of Psychology (Clinical Psychology), Göttingen, Germany
19. Department of Physiology and Pharmacology, Karolinska Institutet, Stockholm, Sweden
20. Departments of Human Genetics and Psychiatry, Donders Institute for Brain, Cognition and Behaviour, Radboud University Medical Center, Nijmegen, The Netherlands
21. Faculty of Health Sciences, Oslo Metropolitan University, Oslo, Norway.
22. Department of Child and Adolescent Psychiatry, University Medical Center Groningen, University of Groningen, Groningen, The Netherlands
23. Interdisciplinary Center Psychopathology and Emotion regulation (ICPE), Department of Psychiatry, University of Groningen, University Medical Center Groningen, Groningen, The Netherlands
24. Division of Molecular Psychiatry, Center of Mental Health, University of Würzburg, Würzburg, Germany.
25. Department of Child and Adolescent Psychiatry, Psychotherapy and Psychosomatics, University Hospital of Würzburg, Würzburg, Germany.
26. Department of Psychiatry and Neuropsychology, School for Mental Health and Neuroscience (MHeNS), Maastricht University, Maastricht, The Netherlands.
27. Data Management, IT Department, University of Oslo, Oslo, Norway
28. Department of Psychology I and Centre of Mental Health, University of Würzburg, Würzburg, Germany
29. Emma Children's Hospital, Amsterdam UMC location University of Amsterdam, Department of Pediatrics, Emma Children's Hospital Amsterdam UMC Follow-Me program & Emma Neuroscience Group, Meibergdreef 9, Amsterdam, The Netherlands
30. Clinical Neuropsychology section, Vrije Universiteit Amsterdam, Amsterdam, The Netherlands
31. Amsterdam Reproduction and Development research institute, Amsterdam, The Netherlands

32. Department of Psychiatry, Psychosomatic Medicine and Psychotherapy, University Hospital Frankfurt, Frankfurt am Main, Germany
33. Hector Institute for Artificial Intelligence in Psychiatry, Central Institute of Mental Health, Medical Faculty Mannheim, Heidelberg University, Mannheim, Germany
34. KG Jebsen Centre for Neurodevelopmental Disorders, University of Oslo, Norway
35. Department of Psychiatry and Psychotherapy, University of Tübingen, Tübingen, Germany

Corresponding Author: V.Mäki-Marttunen, makimarttunen.veronica@gmail.com, Centre for Precision Psychiatry, Institute of Clinical Medicine, University of Oslo & Division of Mental Health and Addiction, Oslo University Hospital, Postboks 4956 Nydalen, 0424 Oslo, TE: +47 23027350

Abstract

The human thalamus is an integrative hub for multiple cortical and subcortical circuits involved in both sensory processing and higher cognitive functions. Group-level thalamic volume differences have been reported for multiple psychiatric and neurological disorders, but previous studies have relied on small samples, covered few disorders, or only investigated the whole thalamus without considering subdivisions. In this multi-site study, we compared thalamic nuclei volumes across several psychiatric and neurological disorders (N = 5 094) and healthy controls (N = 4 552). Using structural MRI scans, we segmented 25 bilateral thalamic nuclei, corresponding to six anatomical groups. We included patients covering 11 clinical conditions including mild cognitive impairment (MCI), dementia (DEM), major depressive disorder, schizophrenia spectrum disorder (SCZ), clinical high risk for schizophrenia, bipolar spectrum disorder, autism spectrum disorder, attention-deficit/hyperactivity disorder, Parkinson's disease, and multiple sclerosis (MS). Linear models revealed that some regions of the thalamus were significantly smaller in several conditions, with largest effects observed for MCI, DEM, SCZ and MS. The thalamic nuclei groups most affected across conditions were the medial and lateral thalamic groups, while the ventral and intralaminar groups were relatively spared. This pattern of effects largely corresponds with the canonical functional subdivision of the thalamus into higher-order and sensory thalamus. Clinical conditions differed when looking at the level of individual nuclei. The results highlight a role for the higher-order thalamus in common brain disorders and a differential involvement at the level of individual nuclei, contributing towards a mechanistic understanding of pathophysiological alteration in the thalamus.

Introduction

Common psychiatric and neurological disorders often display comorbidity (1, 2), substantial symptom overlap (3-7), and at the same time considerable phenotypic and behavioural variability within a single disorder (8, 9), posing a need for cross-diagnostic characterizations (10, 11). Large-scale studies that integrate samples from multiple sites across clinical conditions have the potential to reveal both shared and unique features and mechanisms. Recent trans-diagnostic studies revealed substantial genetic overlap and shared structural and functional brain characteristics across a range of disorders (8, 12-19). However, previous magnetic resonance imaging (MRI) studies on brain structural abnormalities have primarily focused on overall volumes of subcortical structures, and thus the characteristics of subcortical subdivisions in psychiatric and neurological disorders warrants further investigation in a cross-diagnostic setting (20, 21).

The human thalamus comprises multiple nuclei that participate in most aspects of brain function, from modulation of arousal and sensory processing to higher cognitive functions (22-27), and jointly play key roles in multiple cortical and subcortical circuits (28-33). Thalamic structural differences have been reported for multiple psychiatric and neurological disorders relative to healthy controls (34-41). However, most studies assessing thalamic structure in clinical conditions included small samples, covered few disorders, or only investigated the whole thalamus. Recent methodological developments enable automated segmentation of up to 25 bilateral nuclei using structural brain MRI scans (42, 43).

Aiming to discern shared and unique patterns of thalamic abnormalities across neurological and psychiatric disorders, we obtained brain scans from 9 646 individuals from multiple sites and quantified volumes of 25 thalamic nuclei. We compared nuclei volumes across 11 clinical conditions including mild cognitive impairment (MCI), dementia (DEM), Parkinson's disease (PD), multiple sclerosis (MS), major depression (MDD), clinical high-risk for schizophrenia (SCZRISK), schizophrenia spectrum disorder (SCZ), bipolar spectrum disorder (BD), non-SCZ psychosis spectrum diagnoses

(PSYMIX), autism spectrum disorder (ASD), attention-deficit/hyperactivity disorder (ADHD), and healthy controls (HC). In addition to case-control comparisons, we investigated the relation between thalamic nuclei volumes and clinical characteristics, i.e. symptom severity in SCZ and MS and cognitive status in MCI, DEM and HC. To examine possible clinical signatures of changes in thalamic volume, we analysed longitudinal data available from the cohort of MS patients. Finally, to gain a mechanistic understanding of our results, we compared the affected thalamic regions with a known functional characterization, the higher-order thalamic matrix and the thalamic sensory core, based on mRNA expression. Our study highlights the heterogeneity of thalamic subregions and reveals the characteristics of thalamic involvement across psychiatric and neurological disorders.

Methods

Samples and thalamus segmentations

We obtained data from 9 646 individuals (n = 5 094 patients, n = 4 552 HC) through collaborations, data sharing platforms, and in-house samples (see Table 1 and Supplementary Table 1 for sample details). Data collection for each sample was performed with the written informed consent of participants and with approval by the respective local Institutional Review Boards.

Patient group	Number of subjects	Mean age, min-max in years	Sex: f/m
ADHD	641 (ADHD), 931 (HC)	16.6, 7-62 (ADHD), 15.2, 7-61 (HC)	192/449 (ADHD), 462/469 (HC)
ASD	969 (ASD), 1061 (HC)	16.3, 5-64 (ASD), 16.5, 5-54 (HC)	128/841 (ASD), 245/816 (HC)
BD	276 (BD), 935 (HC)	33.6, 16-65 (BD), 33.9, 16-64 (HC)	158/117 (BD), 417/469 (HC)
DEM	828 (DEM), 773 (HC)	74.1, 47-96 (DEM), 72.4, 43-94 (HC)	434/394 (DEM), 431/342 (HC)
MCI	884 (MCI), 745 (HC)	72.3, 38-91 (MCI), 68.9, 38-90 (HC)	362/522 (MCI), 369/376 (HC)
MDD	211 (MDD), 67 (HC)	38.8, 18-71 (MDD), 39.5, 18-64 (HC)	144/67 (MDD), 57/36 (HC)
MS	257 (MS), 603 (HC)	38.4, 18-57 (MS), 34.8, 19-57 (HC)	191/66 (MS), 273/330 (HC)
PD	130 (PD), 67 (HC)	61.2, 38-77 (PD), 60.2, 31-81 (HC)	48/82 (PD), 23/44 (HC)
SCZ	629 (SCZ), 1210 (HC)	33.3, 13-66 (SCZ), 34.2, 12-69 (HC)	206/423 (SCZ), 544/666 (HC)
SCZRISK	73 (SCZ), 42 (HC)	24.2, 18-39 (SCZRISK), 25.6, 19-39 (HC)	22/51 (SCZRISK), 27/15 (HC)
PSYMIX	196 (PSY), 808 (HC)	27.9, 14-56 (PSY), 32.6, 12-57 (HC)	82/114 (PSY), 419/389 (HC)

Table 1. Size and demographic characteristics of the samples, grouped by patient diagnosis. ADHD: attention deficit/hyperactivity disorder; ASD: autism spectrum disorder; BD: bipolar disorder; DEM: dementia; MCI: mild cognitive impairment; MDD: major depressive disorder; MS: multiple sclerosis; PD: Parkinson's disease; SCZ: schizophrenia; SCZRISK: individuals at clinical high-risk for schizophrenia; PSYMIX: non-SCZ psychosis spectrum diagnoses; HC: healthy controls.

For the segmentation of the thalamus, we used T1-weighted three-dimensional brain MRI data. Using Bayesian thalamus segmentation based on ex-vivo MRI and histology in Freesurfer 6.0 (42), we segmented the MRI data into the whole thalamus and 25 bilateral thalamic nuclei (Figure 1). Based on the approach used by previous work including our own (15,41), we grouped the thalamic nuclei into six anatomical thalamic groups: anterior group—the anteroventral nucleus; lateral group—laterodorsal and lateral posterior nucleus; ventral group—ventral anterior, ventral anterior magnocellular, ventral lateral anterior, ventral lateral posterior, ventral posterolateral, and ventromedial nucleus; intralaminar group—central medial, central lateral, paracentral, centromedian, and parafascicular nucleus; medial group—paratenial, reuniens, mediodorsal medial magnocellular, and mediodorsal lateral parvocellular nucleus; and posterior group—the lateral geniculate, medial geniculate, limitans, pulvinar anterior, pulvinar medial, pulvinar lateral, and pulvinar inferior. The thalamic segmentation has high test–retest reliability (most nuclei having intra-class correlation coefficient above 0.90) and is robust to differences in MRI contrast (39, 42), shows good agreement with histological divisions of thalamic nuclei (42), and the six groups have been used in a previous multi-diagnostic study (15). We obtained the volumes in mm^3 for each nuclei group (combining left and right sides), and these data were used for statistical analyses. To further characterize distinct patterns of nuclei abnormalities for each disorder, we also performed statistical analyses at the level of individual nuclei.

Statistical analysis of volumes, brain disorders, and clinical variables

Statistical analyses for group comparisons were conducted using linear regression models in R (R Core Team, 2022). Given that thalamic volume changes over the life span (Sullivan et al. 2004), for each diagnosis we matched controls and patients with respect to mean age and age range. All patient samples had controls scanned on the same scanner with identical MRI sequence parameters. The overall quality of the thalamic segmentation algorithm was assessed through visual inspection of three axial and three coronal slices covering the thalamus of selected cases. Statistical outliers within each diagnostic sample were identified when a volume was smaller or larger than three standard deviations

(n = 65), and their exclusion did not affect the results. For clinical conditions where participants were scanned on multiple scanners, we applied a multivariate scanner harmonization method (**RE**moval of **L**atent **I**nter-scanner **E**ffects through **F**actorization, RELIEF, (44)) that removes scanner-related effects while retaining associations of interest. As an example, Figure S1 shows the decreasing trend of thalamic volume as a function of age for the anterior and posterior groups before and after scanner harmonization.

For each of the clinical conditions, we fitted linear regression models to test for diagnostic group effects on whole thalamic volume as well as volumes of the six thalamic groups. In these models, volumes were entered as dependent variables and diagnosis was the independent variable along with sex, age, age^2 and estimated intracranial volume (ICV, (45)) as covariates (14). The resulting p-values were adjusted for multiple testing (i.e., 6 comparisons, one per thalamic group) using Bonferroni correction. To test for effects that were independent of global thalamic effects, we performed further analyses including whole thalamic volume as an additional covariate. To examine similarities in the patterns of effects found across the different groups, we correlated the patterns of effect sizes of case-control differences across thalamic groups (e.g. rows in Figure 2.b) using Pearson correlations (Figure 3.c).

To explore differences at the level of individual nuclei, we conducted linear regression models on the harmonized data to test for diagnostic group effects on each nucleus, and included sex, age, age^2, ICV, and whole thalamic volume as covariates. We adjusted the statistical threshold using Bonferroni correction (i.e., correcting for 50 comparisons, one per nucleus).

Information concerning illness severity was available for individuals with MCI, DEM, MS, SCZ, and PD. Of these, 1 555 individuals with MCI, 485 individuals with DEM and 1 209 healthy controls had Mini-Mental State Examination (MMSE) score (46), whereas 255 individuals with MS had Expanded Disability Status Scale (EDSS) scores (47). 206 individuals with SCZ had Positive and Negative Syndrome Scale (PANSS) scores (48). Linear regression models were fitted to examine relationships between

clinical variables (i.e., predictors) and thalamic group volumes (i.e., dependent variables), including also ICV, age, age^2 and sex.

While the cross-sectional analysis on the MS sample was conducted using baseline data from the first scanning instance, follow-up data was also available and was employed to investigate the clinical relevance of longitudinal changes on thalamic volume. Different patients participated in one or up to seven sessions (Table S2). For this analysis, data after scanner harmonization applied on all the data and correction for ICV, age, age^2 (at first session) and sex were entered into a linear mixed model using lme4 package (49). We included volume as the dependent variable and years after first session as the variable of interest, and a random effect was included to account for individual differences.

As a final trans-diagnostic analysis, we aimed to provide a low-dimensional description of the shared and unique patterns of thalamic nuclei volume differences relative to healthy controls for each diagnostic group. To assess this, we implemented a dimensionality reduction technique to synthesize the data of thalamic nuclei volumes (i.e. 50 nuclei across left and right hemispheres) across disorders. We first harmonized the data across scanners, including correction for relevant covariates (sex, age, age^2, ICV) as well as whole thalamic volume. We then related the volume of each nucleus for each patient to the corresponding average from the sample's healthy control group, obtaining thus a measure of effect size. Finally, we projected the data onto a low-dimensional space (2-D) using an unsupervised manifold learning algorithm based on topological analysis, the Uniform Manifold Approximation and Projection (UMAP). This analysis was done with the umap toolbox implemented in Python 3.7 (50, 51). The UMAP approach preserves the global data structure and the local neighbour relations better than other existing methods such as Principal Components Analysis, and has been previously used for biological data (52, 53). We plotted separately the density of individuals with the different disorders in the 2-D space. Figure S2 summarizes the pipeline of the UMAP analysis.

This work was performed on the TSD (Tjenester for Sensitive Data) facilities, owned by the University of Oslo, operated and developed by the TSD service group at the University of Oslo, IT-Department (USIT).

RNA Expression analysis

As a comparison for the cross-sectional analysis results, we obtained expression of thalamic matrix marker calbindin-2 and core thalamus marker parvalbumin in humans. RNA expression of these proteins was obtained from the available nuclei at the Human Protein Atlas (www.proteinatlas.org). The thalamic data corresponded to the following labels: anterior ventral nucleus (anterior group); lateral nucleus (lateral group); ventral posterolateral nucleus, ventral posteromedial nucleus, and ventral nuclei (ventral group); centromedian nucleus (intralaminar group); medial dorsal nucleus and nucleus reuniens (medial group); lateral geniculate body, medial geniculate body, posterior nucleus, and pulvinar (posterior group). Expression data of all nuclei within a group were averaged. The inversed expression values were inserted in the correlation matrix of Figure 3.c. As a replication from an independent sample, we obtained RNA expression of calbindin-2 and parvalbumin from the Allen Brain Institute (human.brain-map.org). The thalamic data corresponded to the following labels: ventral anterior, ventral lateral, ventral (ventral group), centromedian (intralaminar group), mediodorsal (medial group), and posterior, posterolateral, lateral geniculate, medial geniculate, pulvinar (posterior group). Data for nuclei in anterior or lateral groups was missing.

Data availability

Data used in the preparation of this article were obtained from the Alzheimer's Disease Neuroimaging Initiative (ADNI) database (adni.loni.usc.edu), PPMI [http://www.ppmi-info.org/], the ABIDE project [https://fcon_1000.projects.nitrc.org/], ADHD200 [http://fcon_1000.projects.nitrc.org/], OASIS [http://www.oasis-brains.org/], SCHIZCONNECT [http://schizconnect.org/] and OpenNeuro (https://openneuro.org/). A detailed overview of the included cohorts and acknowledgement of their respective funding sources and cohort-specific details are provided in Supplementary Table 1.

Results

Case-control comparison of thalamic groups volume

We found larger total thalamic volume in PD, ASD and PSYMIX, with no differences in specific nuclei groups. On the other hand, BD, SCZ and MS showed smaller whole thalamic volume. Figure 2.a-b and Figure 3.a depict the effect sizes and significant case-control differences for each clinical condition. Adjusting for whole thalamic volume, ADHD and ASD presented a larger anterior thalamus. SCZ, DEM, MCI, and MS had smaller lateral and medial thalamic groups and larger ventral and intralaminar groups. In addition, DEM, MCI and MS had smaller anterior group. The smaller lateral and medial thalamic groups in SCZ, DEM, MCI and MS were present with and without adjustment for whole thalamic volume, indicating a regional effect beyond the overall thalamic volume decrease observed in e.g. SCZ and MS. The relative larger ventral and intralaminar thalamic groups found in SCZ, DEM, MCI and MS after correcting for whole thalamic volume largely disappeared without such correction, indicating a relative sparing of these regions with respect to global thalamic effects, rather than an increase in volume in those patient groups. We found no significant case-control differences for MDD or SCZRISK. In sum, in the disorders where specific thalamic groups were affected, volume reductions in the lateral and medial thalamus were most prevalent.

To explore a possible relation between the pattern of volume differences with a known functional characterisation of the thalamus, we obtained the mRNA expression data of two proteins: calbindin-2 (a marker of the thalamic matrix, implicated in the so-called higher-order thalamus) and parvalbumin (a marker of the thalamic core, implicated in sensory functions) (Figure 3.b). We then compared these expression values with the patterns obtained for the different diagnoses. The ~~data suggests that the regional segregation between thalamic matrix and core markers is associated with the~~ nuclei groups that displayed smaller/larger volumes in patient groups were related to the matrix/core thalamus, respectively (Figure 3.c), suggesting the regional segregation between thalamic matrix and core markers as a link between volume abnormalities across different groups~~(Figure 3.c)~~.

Case-control comparison of individual thalamic nuclei volume

To further characterize disease-related thalamic volume changes at higher anatomical resolution, we performed group analyses for the individual nuclei volumes and found distinct patterns of case-control differences for the different clinical conditions. SCZ, MS, MCI and DEM presented the largest number of nuclei with significant case-control differences (Figure 4.b). The results for the different groups showed a high degree of correspondence between the left and right thalamus. Bilateral LGN and the magnocellular part of the medio-dorsal nuclei were the most frequently represented nuclei across disorders (Figure 4.a and c), showing significant case-control differences in five of the 11 conditions. Notably, nuclei belonging to all nuclei groups presented case-control differences in at least some of the clinical conditions. Most of the nuclei that presented no difference between patients and controls belonged to the intralaminar thalamic group (Figure 4.a and c). The correlation between the patterns of case-control analyses (Figure 3.c) was largely concordant when calculating the correlations based on the individual nuclei comparisons, although not for all conditions (Figure S4).

Association between thalamic volume and clinical measures

Models testing for associations between thalamic group volumes and clinical characteristics (Figure 2.c, corrected for sex, age and ICV) revealed a significant relation between MMSE scores and volume of the thalamic groups in DEM and MCI, and in HC, indicating that higher cognitive capacity corresponded to larger volumes, except for the ventral group in MCI and the posterior group in healthy controls, where the correlation was negative. The positive correlation between volume and MMSE was found in the same nuclei groups that significantly differed between DEM/MCI and healthy controls, namely anterior, lateral and ventral groups. We also found a significant correlation between volume of several thalamic groups and EDSS (disability scores) in MS. The nuclei groups that showed significant correlations largely corresponded to the ones that showed case-control differences in MS, i.e., anterior, medial and posterior. Ventral group volumes showed a positive correlation with EDSS. Thalamic group volumes did not show significant association with PANSS scores in patients with SCZ.

Using longitudinal data, we investigated possible changes in thalamic volumes over time in MS. We found a significant decrease in whole thalamus and thalamic nuclei volume with time (Figure 2.c). When correcting for whole thalamic volume, a relative increase was observed for the ventral nuclei group. The change in volume of the whole thalamus and thalamic groups in follow-up sessions (with respect to baseline) was not significantly correlated with differences in EDSS scores between sessions ($p > 0.2$). These results are consistent with a global rather than local atrophy of the thalamus in MS over time.

Low-dimensional representation of thalamic nuclei volume across disorders

To address whether there were patterns in the changes of thalamic volumes when considering all nuclei collectively, we implemented a dimensionality reduction technique (UMAP). This approach allowed us to inspect the distribution of the different clinical groups in a 2-D space define by the two main components. We observed that the patient groups presented distinct patterns of higher density in particular regions of this space (Figure 5, see Figure S5 for annotated density). For instance, the proportion of patients with MS, DEM, MCI and PD was higher for the positive range of the second eigenvector but differed in the position with respect to the first eigenvector. DEM and MCI presented higher density (~38% and ~27%, respectively) at higher values of the second component and around zero values of the first component. MS presented higher density of occurrences (48%) in the upper left quadrant of the 2-D space. PD presented higher density (~36%) for positive values of each component. Some conditions presented a wider distribution, e.g., SCZ. Importantly, the distribution in the 2-D space of healthy older adults was markedly different from those of DEM, MCI, and PD, which had older populations, indicating that age is not driving the observed distribution of groups (Figure S5). Whether the identified clusters (that is, groups with common morphological characteristics) constitute clinically relevant biotypes needs to be explored further. For instance, the region occupied by MS patients is related to overall smaller thalamic volume, including the medial nuclei (magnocellular), while the region occupied by DEM is related to smaller volume in the medial nuclei but a more variable pattern when looking at all the nuclei, with some larger and some smaller than

controls (see Figure S6 for the profiles corresponding to the different sectors of the embedding space). Altogether, the results suggest that the different clinical conditions display differences in the patterns of thalamic nuclei volumetry when considering all nuclei together.

Discussion

In the present study, we analysed 25 bilateral thalamic nuclei volumes in a large dataset comprising patients diagnosed with 11 different psychiatric and neurological conditions. SCZ, DEM, MCI and MS presented significant case-control differences across several nuclei groups. Notably, these differences followed a topological distribution across disorders, such as smaller volumes in anterior, lateral and medial groups, and larger volume in ventral and intralaminar groups. These findings indicate a common involvement of higher-order thalamic nuclei across several brain disorders. Further analyses looking at individual nuclei, including an embedding in a low dimensional space, revealed differences between clinical conditions. Furthermore, we found significant associations between cognition and thalamic volumes in DEM, MCI, and in HC. Our results point both to commonalities and differences across clinical conditions, which are informative to further understand the mechanisms of pathophysiological alterations in the thalamus associated to brain disease.

Thalamic effects across clinical conditions

A main aim and strength of our study was the ability to examine jointly various brain disorders with a unified analytical pipeline. We obtained the results after correction for whole thalamic volume intending to resolve some of the inconsistencies found in the literature regarding thalamic volumes in brain disorders. We found that neurodevelopmental conditions that have onset in childhood (ASD, ADHD) showed a different pattern of volumetric differences (larger volumes) with respect to controls than neurodegenerative or psychiatric disorders with onset later in life (smaller volumes, Figures 2 and 3). We also found consistently lower volumes of the medial and lateral thalamic groups in SCZ, DEM, MCI and MS. These thalamic groups overlap with the so-called *thalamic matrix*, as indicated by expression of the marker protein calbindin (Figure 3, Figure S3). The thalamic matrix is related to

higher order cognitive functions, i.e. “higher order thalamus” (54), in contrast to the *thalamic core* (54, 55), which is mainly associated with sensory relay functions. Further studies including other disorders or longitudinal studies directly assessing the implications of the higher-order versus sensory thalamus are needed, as our results may indicate that this functional subdivision has implications for understanding the comorbidity and symptoms overlap across brain disorders.

Within the medial thalamus, the bilateral medio-dorsal magnocellular nuclei presented significant case-control differences in five of the included disorders. The medio-dorsal nucleus plays an important role in human cognition through its interaction with the prefrontal cortex (56-59), and its impairment has been related to the symptomatology of psychiatric disorders (20, 60, 61). The involvement of the MDm nucleus in a variety of disorders may be related to the cognitive symptoms that are common across ASD, SCZ, DEM, MCI, and MS, and this nucleus may thus be an important target for intervention or focused assessment.

In addition, the bilateral lateral geniculate nuclei (LGN) presented significant effects in many disorders. The LGN is a small nucleus in the posterior part of the thalamus and is part of the core thalamus, relaying information from the retina to the primary visual cortices. Recent studies in rodents have shown that the notion of the core thalamus as a simple “relay station” is too simplistic: activity in LGN can be highly modulated before being conveyed to the cortex (33, 62, 63). The LGN differs functionally from the medio-dorsal magnocellular nuclei that also showed lower volumes across psychiatric and neurological disorders, and the reason why they are both involved in multiple disorders may have different causes. Interestingly, the ventral layer of the LGN receives multiple projections from the higher order thalamus, including the medio-dorsal thalamus (64). One function ascribed to the ventral LGN is associated with circadian rhythms through its projections to the suprachiasmatic nuclei (65-68). Circadian activity and sleep patterns are disrupted in brain disorders (69-71). Here, we did not have the spatial resolution to study structural subdivisions of the LGN, and further studies are

necessary to investigate the role of LGN subregions in the pathophysiology of brain disorders, in particular related to disruption in circadian rhythms.

The dimension reduction analysis revealed specific patterns for each disorder in the components space, and this may be the case also for those conditions where no significant case-control differences were detected at the level of nuclei groups or individual nuclei. Some groups (e.g. SCZ and MDD) occupied larger regions of the 2-D landscape, while others presented higher clustering in one area. For example, neurological disorders such as PD, MS, DEM and MCI tended to cluster on specific and distinct areas of the space, indicating that the patterns of thalamic morphology may be unique for each disorder. While this analysis was exploratory, it suggests that thalamic nuclei volume may present a landscape of variation across common brain disorders that can be exploited to study patient group homogeneity and diagnosis (13).

Thalamic nuclei volumes in clinical conditions

Associations between thalamic volume differences and psychiatric and neurological disorders have previously been reported. However, this is the first study to examine thalamic nuclei groups and individual nuclei across a broad range of psychiatric and neurological conditions, offering new insights into the role of the thalamus in common brain disorders.

We found that DEM and MCI were associated with reduced thalamic volumes across a large portion of the thalamus, with the highest numbers of nuclei in the case-control comparisons, and largely overlapping patterns. Furthermore, we found that in those groups, anterior, lateral and medial thalamic groups volume were positively correlated with cognitive status as measured using MMSE. Interestingly, the volume of the medial group was also correlated with MMSE score in healthy controls, which may indicate a general association of medial thalamic size with cognitive impairments in the elderly population. Our results extend multiple previous studies reporting lower thalamic volumes in Alzheimer's disease and MCI (35, 40), and agree with a recent study using the same thalamic nuclei segmentation approach in a subsample of the data used for this study (n = 45 for

patients) reporting smaller thalamic volumes specifically in mediodorsal and anterior-ventral structures (72). Furthermore, here we show that intralaminar and ventral thalamic groups were spared of this reduction, and that there were distinct patterns to DEM and MCI at the individual nuclei level as compared to the effects observed for other patient groups, indicating spatially localized effects of thalamic morphology for DEM and MCI.

We also found widespread thalamic nuclei groups and nuclei-specific atrophy in MS, spanning anterior, medial, lateral and posterior regions. A significant negative correlation between clinical function (as measured by EDSS) and volume for anterior, medial and posterior thalamic groups indicates that smaller volumes are related to more severe symptoms. The longitudinal analysis showed an overall reduction in whole thalamic volume but no thalamic group-specific effects. As a methodological consideration, we had a decreasing number of scans available for follow-up sessions. However, we ran the longitudinal analysis only for participants that had the same number of sessions (i.e. three sessions, n = 117) and the results remained the same. Reductions in thalamic volume is a well-known marker in MS (38, 73-76), as well as thalamic volume changes over time (77, 78). Our results indicate that anterior, medial, lateral and posterior regions of the thalamus are the most affected in MS and relate to symptom severity, that posterior nuclei reduction may be a unique feature of thalamic morphology in MS, and that an overall reduction of thalamic volume occurs over time after disease onset.

Smaller volumes in medial and lateral groups were also found in SCZ. Interestingly, the case-control comparison at the individual nuclei level and the dimension reduction approach showed different patterns between SCZ and the neurological disorders. Many previous studies reported smaller thalamic volume in SCZ (36, 39, 79, 80) and specifically in the medial and lateral nuclei (81), even at early stages of the disease or in individuals at high risk of developing the disease. Specific thalamic alterations have been suggested to be a hallmark of schizophrenia (41, 82). Our results suggest that delving deeper into these effects may give greater insights in the mechanisms that are both unique

and common along the spectrum of the disorder and those that underlie the heterogeneity of the disease.

In our large sample, we found significantly larger whole thalamic volume in ASD, and larger anterior thalamic group and smaller medial group when controlling for whole thalamic volume. A significant enlargement in ASD has also been reported in a recent study, driven by larger size in posterior regions (83). Our results suggest that this effect may be driven by larger volumes of the lateral pulvinar, as revealed in the case-control analysis at the individual nuclei level (Figure 3.a). We also found an enlargement in the anterior group in ADHD. Larger thalamus in ADHD has been related to higher symptom severity (84). Of note, our samples covered a wide age range (from childhood to adulthood) and age specific effects may have been undetected. Taken together, our large sample and improved thalamic segmentation allowed us to corroborate an enlargement of the thalamus in ASD across the sex and age range, and a specific enlargement of the anterior nuclei in both conditions. The different pattern in ASD and ADHD (i.e., enlargement) compared to DEM, MCI, SCZ and MS, which exhibited predominantly smaller regional thalamic volumes, may be related to the fact that ASD and ADHD tend to appear earlier in life and may therefore be related to aberrant early developmental processes rather than degeneration.

We found smaller thalamic nuclei volume in BD for several nuclei groups including lateral, ventral, medial and posterior. The pattern showed high correlation with the pattern of SCZ (Figure 2.c), however the regional differences in BD were not significant when correcting for whole thalamic volume. A recent study on thalamic nuclei using the same segmentation approach found smaller medial and posterior nuclei in BD (39). Our results are consistent with those findings and suggest that the effects accompany a change in whole thalamic volume.

In contrast to the other neurological conditions, we found moderately larger thalamic volume in PD. This increase was general to the whole thalamus and not specific to a particular nuclei group. Previous results on thalamic volume in PD are variable, in general indicating no significant volumetric

differences but some shape differences between patients and controls (85-87). A recent study (N = 131 patients) reported larger thalamic volume in patients compared to controls (88). Although some heterogeneity has been observed between patients with different sets of symptoms and in different stages of the disease, the evidence points towards either no volume change or a general enlargement of the thalamus as a whole, but not affecting specific nuclei groups in PD.

We found no significant volume differences in MDD and PSYMIX. These groups showed moderate correlations with other conditions at the thalamic groups level (Figure 2.c) and several clusters in the 2-D component space, which may reflect the heterogeneity of these conditions.

Methodological considerations

The current study assessed case-control differences in thalamic nuclei volume in a large sample covering multiple clinical conditions and with a unified pipeline. Some methodological consideration can be identified: 1) We used a thalamus segmentation tool (42) that is currently implemented in FreeSurfer. The segmentation accuracy is known to be limited for some nuclei with weaker signal (72). However, studies comparing the segmentation results of this tool and histological delineation of the thalamus have shown that it is successful in identifying most of the nuclei (42), and in particular medio-dorsal thalamus and LGN have a high reliability (42, 43). Further, high segmentation accuracy has also been reported for this tool in other studies with patient groups (39, 72). Furthermore, we pooled the different nuclei into six thalamic groups, which exhibit high test–retest reliability and which are robust to differences in MRI contrast. 2) Another aspect of our study is that it included data from different scanner sites. We assessed this issue by including patient samples for which a control sample was available from the same scanner. While RELIEF is effective for samples with large number of individuals, it may introduce some variability for sites with few individuals. This may have been the case for some of our smaller samples and the longitudinal analysis, reducing our ability to detect significant results. 3) Patients included in the different studies may have had different medication

status, which was not controlled for in our study. Future studies are necessary to examine the effect of medication on the observed results.

Conclusions

Our results suggest the possibility that a thalamic axis of disruption is found across several disorders with different aetiologies (e.g. psychiatric or neurological), that medial and lateral regions are more vulnerable to disease, and that it is crucial to examine thalamic nuclei separately since opposing effects may be masked when studying the thalamus as a whole. In addition to commonalities, distinct aspects of thalamic morphology were identified for the different conditions, indicating unique aspects of thalamic morphology related to the different disorders. This is the first study to give a comprehensive characterization of thalamic disruption across common brain disorders, and it provides valuable insights that can guide future research and therapeutic strategies.

Acknowledgements

Dr Buitelaar has been supported by the EU-AIMS (European Autism Interventions) and AIMS-2-TRIALS programmes which receive support from Innovative Medicines Initiative Joint Undertaking Grant No. 115300 and 777394, the resources of which are composed of financial contributions from the European Union's FP7 and Horizon2020 Programmes, and from the European Federation of Pharmaceutical Industries and Associations (EFPIA) companies' in-kind contributions, and AUTISM SPEAKS, Autistica and SFARI; and by the Horizon2020 supported programme CANDY Grant No. 847818). The European Research Council under the European Union's Horizon 2020 research and Innovation program (ERC StG Grant No. 802998). The funders had no role in the design of the study; in the collection, analyses, or interpretation of data; in the writing of the manuscript, or in the decision to publish the results. Any views expressed are those of the author(s) and not necessarily those of the funders. Data used in preparation of this article were obtained from the Alzheimer's Disease

Neuroimaging Initiative (ADNI) database (adni.loni.usc.edu). As such, the investigators within the ADNI contributed to the design and implementation of ADNI and/or provided data but did not participate in analysis or writing of this report. A complete listing of ADNI investigators can be found at:

http://adni.loni.usc.edu/wp-content/uploads/how_to_apply/ADNI_Acknowledgement_List.pdf

Supplementary information is available at MP's website.

References

1. Caspi A, Houts RM, Ambler A, Danese A, Elliott ML, Hariri A, et al. Longitudinal Assessment of Mental Health Disorders and Comorbidities Across 4 Decades Among Participants in the Dunedin Birth Cohort Study. JAMA Network Open. 2020;3(4):e203221-e.
2. Plana-Ripoll O, Pedersen CB, Holtz Y, Benros ME, Dalsgaard S, de Jonge P, et al. Exploring Comorbidity Within Mental Disorders Among a Danish National Population. JAMA Psychiatry. 2019;76(3):259-70.
3. Strauss GP, Cohen AS. A transdiagnostic review of negative symptom phenomenology and etiology. Schizophrenia bulletin. 2017;43(4):712-9.
4. Chase TN. Apathy in neuropsychiatric disease: diagnosis, pathophysiology, and treatment. Neurotoxicity research. 2011;19(2):266-78.
5. Gupta R, Advani D, Yadav D, Ambasta RK, Kumar P. Dissecting the relationship between neuropsychiatric and neurodegenerative disorders. Molecular Neurobiology. 2023;60(11):6476-529.
6. Burmeister M, McInnis MG, Zöllner S. Psychiatric genetics: progress amid controversy. Nature Reviews Genetics. 2008;9(7):527-40.
7. Jain R, Maletic V, McIntyre RS. Diagnosing and treating patients with mixed features. The Journal of clinical psychiatry. 2017;78(8):4253.
8. Segal A, Parkes L, Aquino K, Kia SM, Wolfers T, Franke B, et al. Regional, circuit and network heterogeneity of brain abnormalities in psychiatric disorders. Nature Neuroscience. 2023;26(9):1613-29.
9. Young G, Lareau C, Pierre B. One quintillion ways to have PTSD comorbidity: Recommendations for the disordered DSM-5. Psychological Injury and Law. 2014;7:61-74.
10. Fried EI, van Borkulo CD, Cramer AO, Boschloo L, Schoevers RA, Borsboom D. Mental disorders as networks of problems: a review of recent insights. Social psychiatry and psychiatric epidemiology. 2017;52:1-10.
11. Hofmann SG. Toward a cognitive-behavioral classification system for mental disorders. Behavior therapy. 2014;45(4):576-87.
12. Brosch K, Stein F, Schmitt S, Pfarr J-K, Ringwald KG, Thomas-Odenthal F, et al. Reduced hippocampal gray matter volume is a common feature of patients with major depression, bipolar disorder, and schizophrenia spectrum disorders. Molecular Psychiatry. 2022;27(10):4234-43.
13. Okada N, Fukunaga M, Miura K, Nemoto K, Matsumoto J, Hashimoto N, et al. Subcortical volumetric alterations in four major psychiatric disorders: a mega-analysis study of 5604 subjects and a volumetric data-driven approach for classification. Molecular Psychiatry. 2023:1-11.
14. Elvsåshagen T, Bahrami S, van der Meer D, Agartz I, Alnæs D, Barch DM, et al. The genetic architecture of human brainstem structures and their involvement in common brain disorders. Nature communications. 2020;11(1):4016.

15. Elvsåshagen T, Shadrin A, Frei O, van der Meer D, Bahrami S, Kumar VJ, et al. The genetic architecture of the human thalamus and its overlap with ten common brain disorders. Nature communications. 2021;12(1):2909.
16. Radonjić NV, Hess JL, Rovira P, Andreassen O, Buitelaar JK, Ching CR, et al. Structural brain imaging studies offer clues about the effects of the shared genetic etiology among neuropsychiatric disorders. Molecular psychiatry. 2021;26(6):2101-10.
17. Goodkind M, Eickhoff SB, Oathes DJ, Jiang Y, Chang A, Jones-Hagata LB, et al. Identification of a common neurobiological substrate for mental illness. JAMA psychiatry. 2015;72(4):305-15.
18. McTeague LM, Huemer J, Carreon DM, Jiang Y, Eickhoff SB, Etkin A. Identification of common neural circuit disruptions in cognitive control across psychiatric disorders. American Journal of Psychiatry. 2017;174(7):676-85.
19. Young TR, Kumar VJ, Saranathan M. Normative Modeling of Thalamic Nuclear Volumes and Characterization of Lateralized Volume Alterations in Alzheimer's Disease Versus Schizophrenia. Biological Psychiatry: Cognitive Neuroscience and Neuroimaging. 2024.
20. Hwang WJ, Kwak YB, Cho KIK, Lee TY, Oh H, Ha M, et al. Thalamic connectivity system across psychiatric disorders: current status and clinical implications. Biological Psychiatry Global Open Science. 2022;2(4):332-40.
21. Tu P-C, Bai YM, Li C-T, Chen M-H, Lin W-C, Chang W-C, et al. Identification of Common Thalamocortical Dysconnectivity in Four Major Psychiatric Disorders. Schizophrenia Bulletin. 2018;45(5):1143-51.
22. Dolleman-van der Weel MJ, Griffin AL, Ito HT, Shapiro ML, Witter MP, Vertes RP, et al. The nucleus reuniens of the thalamus sits at the nexus of a hippocampus and medial prefrontal cortex circuit enabling memory and behavior. Learning & Memory. 2019;26(7):191.
23. Kawabata K, Bagarinao E, Watanabe H, Maesawa S, Mori D, Hara K, et al. Bridging large-scale cortical networks: Integrative and function-specific hubs in the thalamus. IScience. 2021;24(10).
24. Kumar VJ, Beckmann CF, Scheffler K, Grodd W. Relay and higher-order thalamic nuclei show an intertwined functional association with cortical-networks. Communications Biology. 2022;5(1):1187.
25. Moustafa AA, McMullan RD, Rostron B, Hewedi DH, Haladjian HH. The thalamus as a relay station and gatekeeper: relevance to brain disorders. Reviews in the Neurosciences. 2017;28(2):203-18.
26. Shepherd GM, Yamawaki N. Untangling the cortico-thalamo-cortical loop: cellular pieces of a knotty circuit puzzle. Nature Reviews Neuroscience. 2021;22(7):389-406.
27. Vertes RP, Linley SB, Rojas AK. Structural and functional organization of the midline and intralaminar nuclei of the thalamus. Frontiers in Behavioral Neuroscience. 2022;16:964644.
28. Acsády L. The thalamic paradox. Nature neuroscience. 2017;20(7):901-2.
29. Bolkan SS, Stujenske JM, Parnaudeau S, Spellman TJ, Rauffenbart C, Abbas AI, et al. Thalamic projections sustain prefrontal activity during working memory maintenance. Nature neuroscience. 2017;20(7):987-96.
30. Hwang K, Bertolero MA, Liu WB, D'Esposito M. The human thalamus is an integrative hub for functional brain networks. Journal of Neuroscience. 2017;37(23):5594-607.
31. Nakajima M, Halassa MM. Thalamic control of functional cortical connectivity. Current opinion in neurobiology. 2017;44:127-31.
32. Schmitt LI, Wimmer RD, Nakajima M, Happ M, Mofakham S, Halassa MM. Thalamic amplification of cortical connectivity sustains attentional control. Nature. 2017;545(7653):219-23.
33. Sherman SM. Thalamus plays a central role in ongoing cortical functioning. Nature neuroscience. 2016;19(4):533-41.
34. Adriano F, Spoletini I, Caltagirone C, Spalletta G. Updated meta-analyses reveal thalamus volume reduction in patients with first-episode and chronic schizophrenia. Schizophrenia research. 2010;123(1):1-14.

35. Biesbroek JM, Verhagen MG, van der Stigchel S, Biessels GJ. When the central integrator disintegrates: A review of the role of the thalamus in cognition and dementia. Alzheimer's & Dementia. 2023.
36. Huang A, Rogers B, Sheffield J, Jalbrzikowski M, Anticevic A, Blackford J, et al. Thalamic Nuclei Volumes in Psychotic Disorders and Youth With Psychosis Spectrum Symptoms. Biological Psychiatry. 2020;87(9):S447.
37. Jiang Y, Patton MH, Zakharenko SS. A case for thalamic mechanisms of schizophrenia: perspective from modeling 22q11. 2 deletion syndrome. Frontiers in Neural Circuits. 2021;15:769969.
38. Minagar A, Barnett MH, Benedict RH, Pelletier D, Pirko I, Sahraian MA, et al. The thalamus and multiple sclerosis: modern views on pathologic, imaging, and clinical aspects. Neurology. 2013;80(2):210-9.
39. Mørch-Johnsen L, Jørgensen KN, Barth C, Nerland S, Bringslid IK, Wortinger LA, et al. Thalamic nuclei volumes in schizophrenia and bipolar spectrum disorders–Associations with diagnosis and clinical characteristics. Schizophrenia Research. 2023;256:26-35.
40. Power BD, Looi JC. The thalamus as a putative biomarker in neurodegenerative disorders. Australian & New Zealand Journal of Psychiatry. 2015;49(6):502-18.
41. Steullet P. Thalamus-related anomalies as candidate mechanism-based biomarkers for psychosis. Schizophrenia research. 2020;226:147-57.
42. Iglesias JE, Insausti R, Lerma-Usabiaga G, Bocchetta M, Van Leemput K, Greve DN, et al. A probabilistic atlas of the human thalamic nuclei combining ex vivo MRI and histology. Neuroimage. 2018;183:314-26.
43. Su JH, Thomas FT, Kasoff WS, Tourdias T, Choi EY, Rutt BK, et al. Thalamus Optimized Multi Atlas Segmentation (THOMAS): fast, fully automated segmentation of thalamic nuclei from structural MRI. Neuroimage. 2019;194:272-82.
44. Zhang R, Oliver LD, Voineskos AN, Park JY. RELIEF: A structured multivariate approach for removal of latent inter-scanner effects. Imaging Neuroscience. 2023;1:1-16.
45. Buckner RL, Head D, Parker J, Fotenos AF, Marcus D, Morris JC, et al. A unified approach for morphometric and functional data analysis in young, old, and demented adults using automated atlas-based head size normalization: reliability and validation against manual measurement of total intracranial volume. Neuroimage. 2004;23(2):724-38.
46. Cockrell JR, Folstein MF. Mini-mental state examination. Principles and practice of geriatric psychiatry. 2002:140-1.
47. Kurtzke JF. Rating neurologic impairment in multiple sclerosis: an expanded disability status scale (EDSS). Neurology. 1983;33(11):1444-.
48. Kay SR, Fiszbein A, Opler LA. The positive and negative syndrome scale (PANSS) for schizophrenia. Schizophrenia bulletin. 1987;13(2):261-76.
49. Bates D, Mächler M, Bolker B, Walker S. Fitting linear mixed-effects models using lme4. arXiv preprint arXiv:14065823. 2014.
50. Abraham A, Pedregosa F, Eickenberg M, Gervais P, Mueller A, Kossaifi J, et al. Machine learning for neuroimaging with scikit-learn. Frontiers in neuroinformatics. 2014;8:14.
51. Dorrity MW, Saunders LM, Queitsch C, Fields S, Trapnell C. Dimensionality reduction by UMAP to visualize physical and genetic interactions. Nature communications. 2020;11(1):1537.
52. Zerbi V, Pagani M, Markicevic M, Matteoli M, Pozzi D, Fagiolini M, et al. Brain mapping across 16 autism mouse models reveals a spectrum of functional connectivity subtypes. Molecular psychiatry. 2021;26(12):7610-20.
53. Becht E, McInnes L, Healy J, Dutertre C-A, Kwok IW, Ng LG, et al. Dimensionality reduction for visualizing single-cell data using UMAP. Nature biotechnology. 2019;37(1):38-44.
54. Jones EG. The thalamic matrix and thalamocortical synchrony. Trends in neurosciences. 2001;24(10):595-601.

55. Jones EG. Synchrony in the interconnected circuitry of the thalamus and cerebral cortex. Annals of the New York Academy of Sciences. 2009;1157(1):10-23.
56. Parnaudeau S, Bolkan SS, Kellendonk C. The mediodorsal thalamus: an essential partner of the prefrontal cortex for cognition. Biological psychiatry. 2018;83(8):648-56.
57. Pergola G, Danet L, Pitel A-L, Carlesimo GA, Segobin S, Pariente J, et al. The regulatory role of the human mediodorsal thalamus. Trends in cognitive sciences. 2018;22(11):1011-25.
58. Mitchell AS, Chakraborty S. What does the mediodorsal thalamus do? Frontiers in systems neuroscience. 2013;7:37.
59. Georgescu IA, Popa D, Zagrean L. The anatomical and functional heterogeneity of the mediodorsal thalamus. Brain Sciences. 2020;10(9):624.
60. Alelú-Paz R, Giménez-Amaya JM. The mediodorsal thalamic nucleus and schizophrenia. Journal of Psychiatry and Neuroscience. 2008;33(6):489-98.
61. Benoit LJ, Canetta S, Kellendonk C. Thalamocortical development: a neurodevelopmental framework for schizophrenia. Biological psychiatry. 2022;92(6):491-500.
62. Molnár B, Sere P, Bordé S, Koós K, Zsigri N, Horváth P, et al. Cell type-specific arousal-dependent modulation of thalamic activity in the lateral geniculate nucleus. Cerebral Cortex Communications. 2021;2(2):tgab020.
63. Spacek MA, Crombie D, Bauer Y, Born G, Liu X, Katzner S, et al. Robust effects of corticothalamic feedback and behavioral state on movie responses in mouse dLGN. Elife. 2022;11:e70469.
64. Kolmac CI, Power BD, Mitrofanis J. Dorsal thalamic connections of the ventral lateral geniculate nucleus of rats. Journal of Neurocytology. 2000;29:31-41.
65. Pu M, Pickard GE. Ventral lateral geniculate nucleus afferents to the suprachiasmatic nucleus in the cat. Brain research. 1996;725(2):247-51.
66. Harrington ME. The ventral lateral geniculate nucleus and the intergeniculate leaflet: interrelated structures in the visual and circadian systems. Neuroscience & Biobehavioral Reviews. 1997;21(5):705-27.
67. Zhang D, Rusak B. Photic sensitivity of geniculate neurons that project to the suprachiasmatic nuclei or the contralateral geniculate. Brain research. 1989;504(1):161-4.
68. Monavarfeshani A, Sabbagh U, Fox MA. Not a one-trick pony: Diverse connectivity and functions of the rodent lateral geniculate complex. Visual neuroscience. 2017;34:E012.
69. Jones SG, Benca RM. Circadian disruption in psychiatric disorders. Sleep medicine clinics. 2015;10(4):481-93.
70. Walker WH, Walton JC, DeVries AC, Nelson RJ. Circadian rhythm disruption and mental health. Translational psychiatry. 2020;10(1):28.
71. Alachkar A, Lee J, Asthana K, Vakil Monfared R, Chen J, Alhassen S, et al. The hidden link between circadian entropy and mental health disorders. Translational psychiatry. 2022;12(1):281.
72. Tregidgo HF, Soskic S, Althonayan J, Maffei C, Van Leemput K, Golland P, et al. Accurate Bayesian segmentation of thalamic nuclei using diffusion MRI and an improved histological atlas. NeuroImage. 2023;274:120129.
73. Kipp M, Wagenknecht N, Beyer C, Samer S, Wuerfel J, Nikoubashman O. Thalamus pathology in multiple sclerosis: from biology to clinical application. Cellular and molecular life sciences. 2015;72:1127-47.
74. Cifelli A, Arridge M, Jezzard P, Esiri MM, Palace J, Matthews PM. Thalamic neurodegeneration in multiple sclerosis. Annals of Neurology: Official Journal of the American Neurological Association and the Child Neurology Society. 2002;52(5):650-3.
75. Rocca MA, Mesaros S, Pagani E, Sormani MP, Comi G, Filippi M. Thalamic damage and long-term progression of disability in multiple sclerosis. Radiology. 2010;257(2):463-9.
76. Amin M, Ontaneda D. Thalamic injury and cognition in multiple sclerosis. Frontiers in Neurology. 2021;11:623914.

77. Schoonheim MM, Hulst HE, Brandt RB, Strik M, Wink AM, Uitdehaag BM, et al. Thalamus structure and function determine severity of cognitive impairment in multiple sclerosis. Neurology. 2015;84(8):776-83.
78. Houtchens M, Benedict R, Killiany R, Sharma J, Jaisani Z, Singh B, et al. Thalamic atrophy and cognition in multiple sclerosis. Neurology. 2007;69(12):1213-23.
79. Dorph-Petersen K-A, Lewis DA. Postmortem structural studies of the thalamus in schizophrenia. Schizophrenia Research. 2017;180:28-35.
80. Huang AS, Kang K, Vandekar S, Rogers BP, Heckers S, Woodward ND. Lifespan development of thalamic nuclei and characterizing thalamic nuclei abnormalities in schizophrenia using normative modeling. Neuropsychopharmacology. 2024:1-10.
81. Thalhammer M, Schulz J, Scheulen F, Oubaggi MEM, Kirschner M, Kaiser S, et al. Distinct Volume Alterations of Thalamic Nuclei Across the Schizophrenia Spectrum. Schizophrenia Bulletin. 2024;50(5):1208-22.
82. Pergola G, Selvaggi P, Trizio S, Bertolino A, Blasi G. The role of the thalamus in schizophrenia from a neuroimaging perspective. Neuroscience & Biobehavioral Reviews. 2015;54:57-75.
83. Schuetze M, Park MTM, Cho IY, MacMaster FP, Chakravarty MM, Bray SL. Morphological alterations in the thalamus, striatum, and pallidum in autism spectrum disorder. Neuropsychopharmacology. 2016;41(11):2627-37.
84. Fu C, Chen S, Qian A, Zhou R, Zhou J, Li J, et al. Larger thalamus correlated with inattentive severity in the inattentive subtype of ADHD without comorbidity. Psychiatry Research. 2021;304:114079.
85. Garg A, Appel-Cresswell S, Popuri K, McKeown MJ, Beg MF. Morphological alterations in the caudate, putamen, pallidum, and thalamus in Parkinson's disease. Frontiers in neuroscience. 2015;9:101.
86. Lee S, Kim SS, Tae W, Lee S, Choi J, Koh S, et al. Regional volume analysis of the Parkinson disease brain in early disease stage: gray matter, white matter, striatum, and thalamus. American Journal of Neuroradiology. 2011;32(4):682-7.
87. McKeown MJ, Uthama A, Abugharbieh R, Palmer S, Lewis M, Huang X. Shape (but not volume) changes in the thalami in Parkinson disease. BMC neurology. 2008;8(1):1-8.
88. Chen Y, Zhu G, Liu D, Liu Y, Yuan T, Zhang X, et al. The morphology of thalamic subnuclei in Parkinson's disease and the effects of machine learning on disease diagnosis and clinical evaluation. Journal of the neurological sciences. 2020;411:116721.

Figure Legends

Figure 1. Example of the segmentation of the thalamus of one individual into 50 different nuclei (25 for each hemisphere). LD: latero-dorsal; AV: anteroventral; VLa: ventral lateral anterior; VLp: ventral lateral posterior; VPL: ventral posterolateral; LP: lateral posterior; MDm: medio-dorsal magnocellular; VA: ventral anterior; MDl: mediodorsal lateral; CeM: centro-median; PuA: pulvinar anterior; PuM: pulvinar medial; PuL: pulvinar lateral; PuI: pulvinar inferior; Sg: suprageniculate; Pf: parafascicular ; MGN: medial geniculate nucleus; LGN: lateral geniculate nucleus.

Figure 2. a-b) Thalamic volumetric differences between patients and healthy controls (HC). Numbers indicate Cohen's d for the patients versus HC analysis. a) Results for the thalamic groups without adjustment for whole thalamic volume. b) Results for the thalamic groups after adjustment for whole thalamic volume. Data harmonized for scanning site and corrected for total ICV, age, age^2 and sex. c) Coefficients of linear regression between thalamic groups volume and clinical variables. Cells coloured in red indicate significant positive associations and cells in blue indicate significant negative associations. ADHD: attention deficit/hyperactivity disorder; ASD: autism spectrum disorder; BD: bipolar disorder; DEM: dementia; MCI: mild cognitive impairment; MDD: major depressive disorder; MS: multiple sclerosis; PD: Parkinson's disease; SCZ: schizophrenia; SCZRISK: individuals at clinical high-risk for schizophrenia; PSYMIX: non-SCZ psychosis spectrum diagnoses; MMSE: Mini-Mental State Examination; EDSS: Extended Disability Status Scale; PANSS: Positive and Negative Syndrome Scale.

Figure 3. a) Illustration of thalamic groups in the axial plane presenting significant volumetric differences between patients and controls, as shown in Figure 2.b. Results were calculated collapsing the data for left and right hemispheres, and thus only one side is shown. Colorbar indicates Cohen's d. b) Expression of thalamic matrix marker calbindin-2 (left) and core thalamus marker parvalbumin (right) in humans. The colour code indicates the degree of expression within each nuclei group, normalized by the total expression of the protein over the whole thalamus. See also Figure S3 for the expression distribution from an independent dataset (Allen Brain Institute). c) Correlation matrix of thalamic group effects across disorders. Larger correlations indicate more similar patterns of case-control differences in thalamic nuclei groups (rows in Figure 2.b). Expression of calbindin-2 and parvalbumin are added as rows, such as larger correlation indicates larger concordance with the case-control pattern of disruption (rows in Figure 2.b). Colorbar indicates correlation value. For a similar correlation approach at the level of individual nuclei, see Figure S4. ADHD: attention deficit/hyperactivity disorder; ASD: autism spectrum disorder; BD: bipolar disorder; DEM: dementia; MCI: mild cognitive impairment; MDD: major depressive disorder; MS: multiple sclerosis; PD: Parkinson's disease; SCZ: schizophrenia; SCZRISK: individuals at clinical high-risk for schizophrenia; PSYMIX: non-SCZ psychosis spectrum diagnoses; Ca: calbindin-2; PVB: parvalbumin; A: anterior; V: ventral; L: lateral; M: medial; P: posterior; Int.: intralaminar.

Figure 4. a) Individual thalamic nuclei presenting significant case-control differences, adjusting by whole thalamic volume and relevant covariates. Red indicates larger volume in patients, blue indicates smaller volume. b) Percentage of individual nuclei presenting significant case-controls differences for the different clinical conditions. c) Number of clinical conditions showing a significant case-control difference ("disease index") after Bonferroni correction. Zero indicates nuclei with no significant differences. Colours indicate thalamic groups. ADHD: attention deficit and hyperactivity disorder; ASD:

autism spectrum disorder; BD: bipolar disorder; DEM: dementia; MCI: mild cognitive impairment; MDD: major depressive disorder; MS: multiple sclerosis; PD: Parkinson's disease; SCZ: schizophrenia; SCZRISK: individuals at clinical high-risk for schizophrenia; PSYMIX: non-SCZ psychosis spectrum diagnoses; LD: latero-dorsal; AV: anteroventral; VAmc: ventral anterior magnocellular; VLa: ventral lateral anterior; VLp: ventral lateral posterior; VPL: ventral posterolateral; LP: lateral posterior; MDm: medio-dorsal magnocellular; VA: ventral anterior; VM: ventromedial; CL: central lateral; Pc: paracentral; Pt: paratenial; MDl: mediodorsal lateral; CeM: centro-median; PuA: pulvinar anterior; PuM: pulvinar medial; PuL: pulvinar lateral; PuI: pulvinar inferior; Sg: suprageniculate; Pf: parafascicular ; MGN: medial geniculate nucleus; LGN: lateral geniculate nucleus; LH: left hemisphere; RH: right hemisphere.

Figure 5. Embedding of all brain disorders in the 2-components space after UMAP dimensionality reduction of the individual thalamic nuclei effects. Colour scale and contours represent the density of occurrences in each area of the 2-D space. Data from each individual for the clinical groups was normalized to the average sample's healthy control group and were submitted to the UMAP algorithm. ADHD: attention deficit and hyperactivity disorder; ASD: autism spectrum disorder; BD: bipolar disorder; DEM: dementia; MCI: mild cognitive impairment; MDD: major depressive disorder; MS: multiple sclerosis; PD: Parkinson's disease; SCZ: schizophrenia; SCZRISK: individuals at clinical high-risk for schizophrenia; PSYMIX: non-SCZ psychosis spectrum diagnoses.

Tables

Patient group	Number of subjects	Mean age, min-max in years	Sex: %f / %m
ADHD	641 (ADHD), 931 (HC)	16.6, 7-62 (ADHD), 15.2, 7-61 (HC)	30/70 (ADHD), 50/50 (HC)
ASD	969 (ASD), 1061 (HC)	16.3, 5-64 (ASD), 16.5, 5-54 (HC)	13/87 (ASD), 23/77 (HC)
BD	276 (BD), 935 (HC)	33.6, 16-65 (BD), 33.9, 16-64 (HC)	57/43 (BD), 50/50 (HC)
DEM	828 (DEM), 773 (HC)	74.1, 47-96 (DEM), 72.4, 43-94 (HC)	52/48 (DEM), 56/44 (HC)
MCI	884 (MCI), 745 (HC)	72.3, 38-91 (MCI), 68.9, 38-90 (HC)	41/59 (MCI), 50/50 (HC)
MDD	211 (MDD), 67 (HC)	38.8, 18-71 (MDD), 39.5, 18-64 (HC)	68/32 (MDD), 61/39 (HC)
MS	257 (MS), 603 (HC)	38.4, 18-57 (MS), 34.8, 19-57 (HC)	74/26 (MS), 45/55 (HC)
PD	130 (PD), 67 (HC)	61.2, 38-77 (PD), 60.2, 31-81 (HC)	37/63 (PD), 34/66 (HC)
SCZ	629 (SCZ), 1210 (HC)	33.3, 13-66 (SCZ), 34.2, 12-69 (HC)	33/67 (SCZ), 45/55 (HC)
SCZRISK	73 (SCZ), 42 (HC)	24.2, 18-39 (SCZRISK), 25.6, 19-39 (HC)	30/70 (SCZRISK), 64/36 (HC)
PSYMIX	196 (PSY), 808 (HC)	27.9, 14-56 (PSY), 32.6, 12-57 (HC)	42/58 (PSY), 52/48 (HC)

Table 1. Size and demographic characteristics of the samples, grouped by patient diagnosis. ADHD: attention deficit/hyperactivity disorder; ASD: autism spectrum disorder; BD: bipolar disorder; DEM: dementia; MCI: mild cognitive impairment; MDD: major depressive disorder; MS: multiple sclerosis; PD: Parkinson's disease; SCZ: schizophrenia; SCZRISK: individuals at clinical high-risk for schizophrenia; PSYMIX: non-SCZ psychosis spectrum diagnoses; HC: healthy controls.

Figures

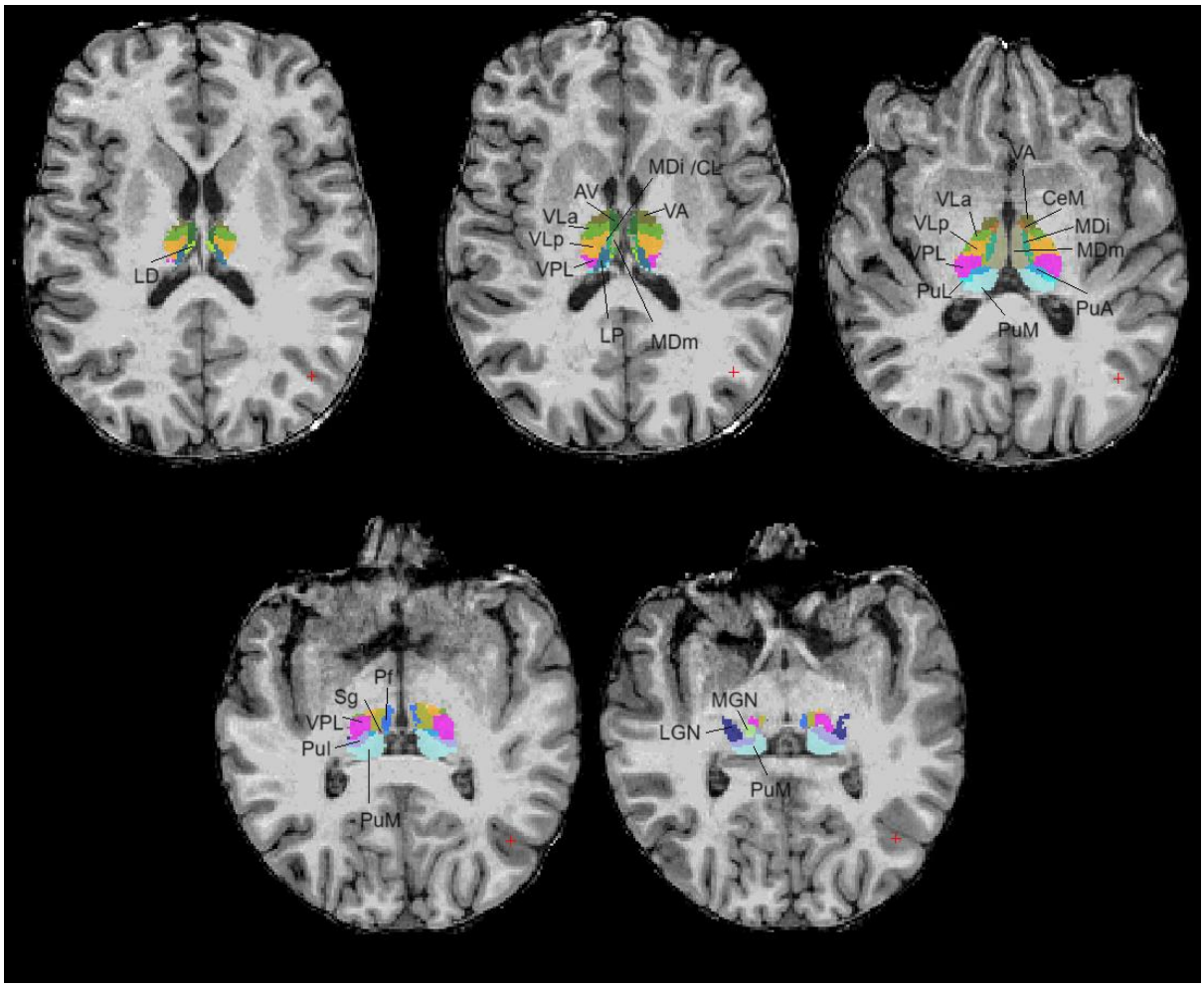

Figure 1. Example of the segmentation of the thalamus of one individual into 50 different nuclei (25 for each hemisphere). LD: latero-dorsal; AV: anteroventral; VLa: ventral lateral anterior; VLp: ventral lateral posterior; VPL: ventral posterolateral; LP: lateral posterior; MDm: medio-dorsal magnocellular; VA: ventral anterior; MDl: mediodorsal lateral; CeM: centro-median; PuA: pulvinar anterior; PuM: pulvinar medial; PuL: pulvinar lateral; PuI: pulvinar inferior; Sg: suprageniculate; Pf: parafascicular ; MGN: medial geniculate nucleus; LGN: lateral geniculate nucleus.

a) Case-control results - Not correcting for whole thalamic volume

Diagnosis	ICV	Whole thalamus	Anterior	Lateral	Medial	Ventral	Intralaminar	Posterior
MDD	-0.09	-0.1	-0.02	0.04	-0.10	-0.10	-0.10	-0.08
PSYMIX	-0.04	0.2	0.12	0.07	0.18	0.18	0.15	0.20
PD	0.25	0.34	0.13	0.11	0.32	0.33	0.34	0.31
SCZ-risk	0.37	0.21	0.10	0.08	0.08	0.18	0.15	0.28
BD	-0.06	-0.23	-0.17	-0.23	-0.22	-0.19	-0.16	-0.25
ADHD	0.31	0.09	0.17	0.08	0.03	0.10	0.13	0.07
ASD	0.18	0.11	0.20	0.05	0.01	0.10	0.09	0.14
SCZ	0.06	-0.15	-0.06	-0.22	-0.26	-0.10	-0.04	-0.15
DEM	0.08	0	-0.30	-0.23	-0.42	0.09	0.14	0.05
MCI	0.22	0.05	-0.17	-0.14	-0.23	0.14	0.16	0.05
MS	-0.20	-0.31	-0.51	-0.44	-0.56	0.06	-0.02	-0.63

b) Case-control results – Correcting for whole thalamic volume

Diagnosis	ICV	Whole thalamus	Anterior	Lateral	Medial	Ventral	Intralaminar	Posterior
MDD	-0.09	-0.1	0.07	0.11	-0.03	-0.02	-0.03	0.01
PSYMIX	-0.04	0.2	-0.02	-0.09	0.03	-0.03	-0.07	0.04
PD	0.25	0.34	-0.22	-0.34	0.07	0.01	0.05	0.00
SCZ-risk	0.37	0.21	-0.05	-0.07	-0.14	-0.07	-0.10	0.19
BD	-0.06	-0.23	0.01	-0.09	-0.04	0.12	0.11	-0.11
ADHD	0.31	0.09	0.20	0.01	-0.11	0.05	0.14	-0.04
ASD	0.18	0.11	0.19	-0.04	-0.18	-0.02	-0.02	0.10
SCZ	0.06	-0.15	0.10	-0.17	-0.25	0.18	0.26	-0.03
DEM	0.08	0	-0.33	-0.27	-0.57	0.34	0.33	0.16
MCI	0.22	0.05	-0.22	-0.20	-0.39	0.31	0.28	0.00
MS	-0.2	-0.31	-0.39	-0.31	-0.50	1.10	0.63	-0.76

Cohen's d

Patients larger than HC	*Patients smaller than HC*
0 - 0.3	0 - 0.3
0.3 - 0.5	0.3 - 0.5
> 0.5	> 0.5

c) Correlations with clinical variables

	Score (mean/min/max)	Whole thalamus	Anterior	Lateral	Medial	Ventral	Intralaminar
MMSE							
DEM	**22** / 4 / 30	-0.04	0.17	0.12	0.12	-0.08	0.03
MCI	**27** / 3 / 30	0.07	0.07	0.06	0.12	-0.07	-0.02
HC	**29** / 19 / 30	0.01	0.02	-0.01	0.13	0.00	-0.03
EDSS							
MS	**1.88** / 0.00 / 7.00	0.00	-0.13	-0.12	-0.14	0.25	-0.06
PANSS							
SCZ – general	**29** / 16 / 69	-0.10	-0.06	0.12	-0.09	-0.01	0.12
SCZ – positive	**14** / 7 / 34	-0.10	0.03	0.12	-0.11	0.09	0.09
SCZ – negative	**15** / 7 / 43	-0.13	-0.12	-0.11	0.08	-0.01	0.00
Longitudinal							
MS							
time effect		-54.00	-1.44	-1.34	-10.37	-18.86	-2.48
time effect (corr.WT)			-0.30	-0.06	-2.40	6.00	0.68

p value

Positive	*Negative*
<0.05	<0.05
<0.001	<0.001
<0.00001	<0.00001

Figure 2. a-b) Thalamic volumetric differences between patients and healthy controls. Numbers indicate Cohen's d for the patients versus HC analysis. a) Results for the thalamic groups without adjustment for whole thalamic volume. b) Results for the thalamic groups after adjustment for whole thalamic volume. Data corrected for scanning site, total ICV, age, age^2 and sex. c) Coefficients of linear regression between thalamic groups volume and clinical variables. Cells coloured in red indicate

significant positive associations and cells in blue indicate significant negative associations. ADHD: attention deficit/hyperactivity disorder; ASD: autism spectrum disorder; BD: bipolar disorder; DEM: dementia; MCI: mild cognitive impairment; MDD: major depressive disorder; MS: multiple sclerosis; PD: Parkinson's disease; SCZ: schizophrenia; SCZRISK: individuals at clinical high-risk for schizophrenia; PSYMIX: non-SCZ psychosis spectrum diagnoses; HC: healthy controls; MMSE: Mini-Mental State Examination; EDSS: Extended Disability Status Scale; PANSS: Positive and Negative Syndrome Scale.

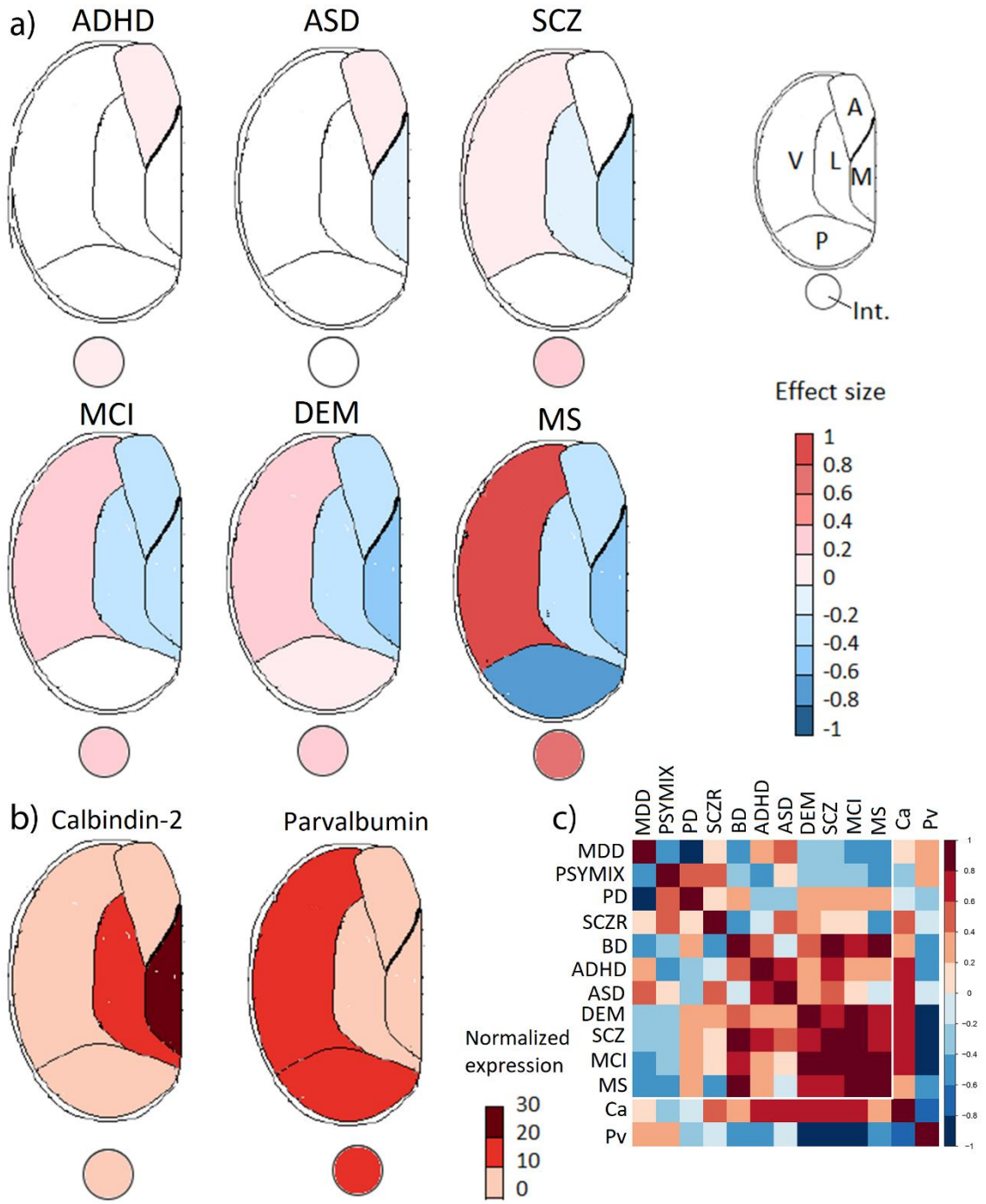

Figure 3. a) Illustration of thalamic groups in the axial plane presenting significant volumetric differences between patients and controls, as shown in Figure 2.b. Results were calculated collapsing the data for left and right hemispheres, and thus only one side is shown. Colorbar indicates Cohen's d. b) Expression of thalamic matrix marker calbindin-2 (left) and core thalamus marker parvalbumin (right) in humans. The colour code indicates the degree of expression within each nuclei group, normalized by the total expression of the protein over the whole thalamus. See also Figure S3 for the expression distribution

from an independent dataset (Allen Brain Institute). c) Correlation matrix of thalamic group effects across disorders. Larger correlations indicate more similar patterns of case-control differences in thalamic nuclei groups (rows in Figure 2.b). Expression of calbindin-2 and parvalbumin are added as rows, such as larger correlation indicates larger concordance with the case-control pattern of disruption (rows in Figure 2.b). Colorbar indicates correlation value. For a similar correlation approach at the level of individual nuclei, see Figure S4. ADHD: attention deficit/hyperactivity disorder; ASD: autism spectrum disorder; BD: bipolar disorder; DEM: dementia; MCI: mild cognitive impairment; MDD: major depressive disorder; MS: multiple sclerosis; PD: Parkinson's disease; SCZ: schizophrenia; SCZRISK: individuals at clinical high-risk for schizophrenia; PSYMIX: non-SCZ psychosis spectrum diagnoses; Ca: calbindin-2; PVB: parvalbumin; A: anterior; V: ventral; L: lateral; M: medial; P: posterior; Int.: intralaminar.

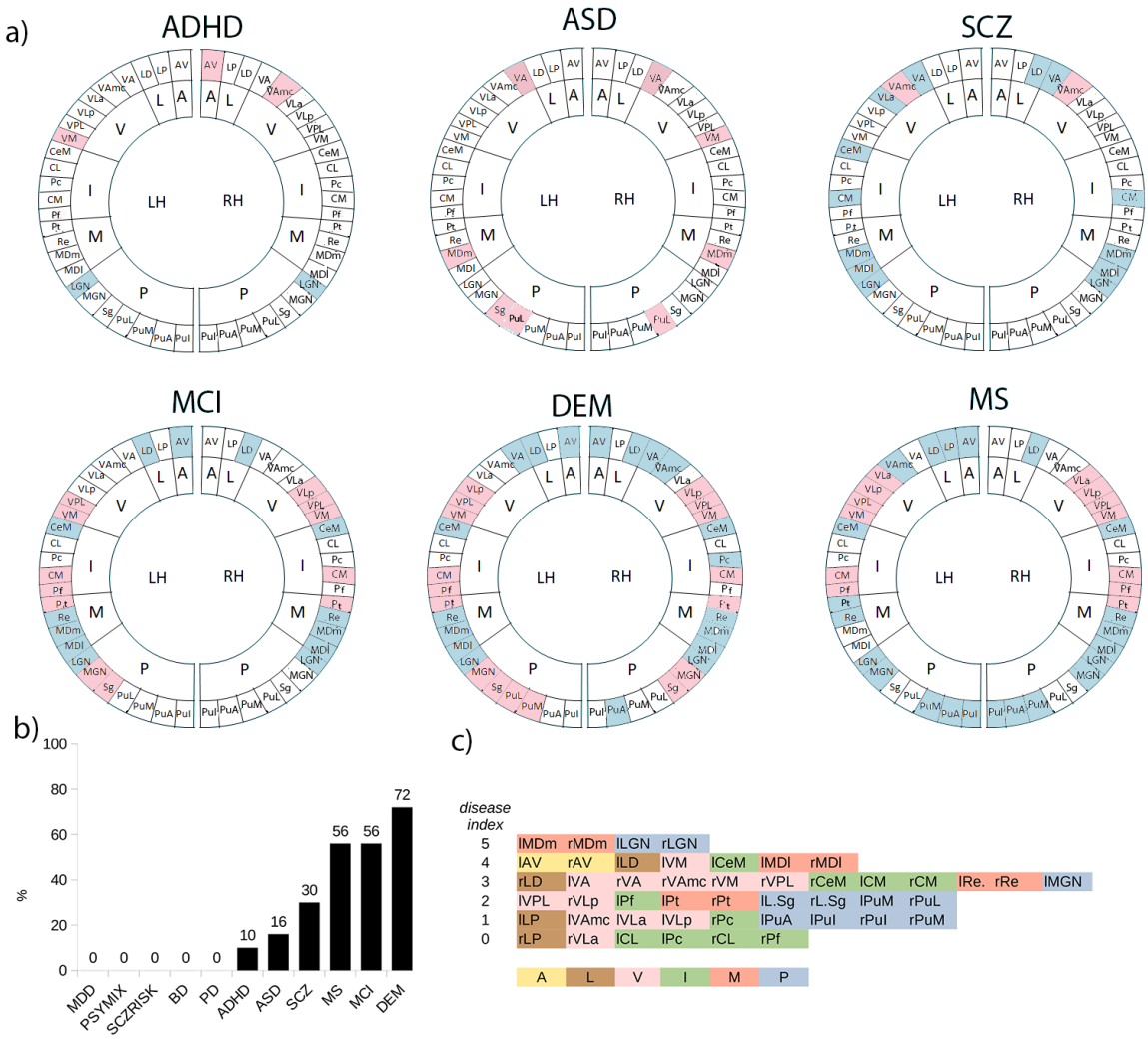

Figure 4. a) Individual thalamic nuclei presenting significant case-control differences, adjusting by whole thalamic volume and relevant covariates. Red indicates larger volume in patients, blue indicates smaller volume. b) Percentage of individual nuclei presenting significant case-controls differences for the different clinical conditions. c) Number of clinical conditions showing a significant case-control difference ("disease index") after Bonferroni correction. Zero indicates nuclei with no significant differences. Colours indicate thalamic groups. ADHD: attention deficit and hyperactivity disorder; ASD: autism spectrum disorder; BD: bipolar disorder; DEM: dementia; MCI: mild cognitive impairment; MDD: major depressive disorder; MS: multiple sclerosis; PD: Parkinson's disease; SCZ: schizophrenia; SCZRISK: individuals at clinical high-risk for schizophrenia; PSYMIX: non-SCZ psychosis spectrum diagnoses; LD: latero-dorsal; AV: anteroventral; VAmc: ventral anterior magnocellular; VLa: ventral lateral anterior; VLp: ventral lateral posterior; VPL: ventral posterolateral; LP: lateral posterior; MDm: medio-dorsal magnocellular; VA: ventral anterior; VM: ventromedial; CL: central lateral; Pc: paracentral; Pt: paratenial; MDl: mediodorsal lateral; CeM: centro-median; PuA: pulvinar anterior; PuM: pulvinar medial; PuL: pulvinar lateral; Pul: pulvinar

inferior; Sg: suprageniculate; Pf: parafascicular ; MGN: medial geniculate nucleus; LGN: lateral geniculate nucleus; LH: left hemisphere; RH: right hemisphere.

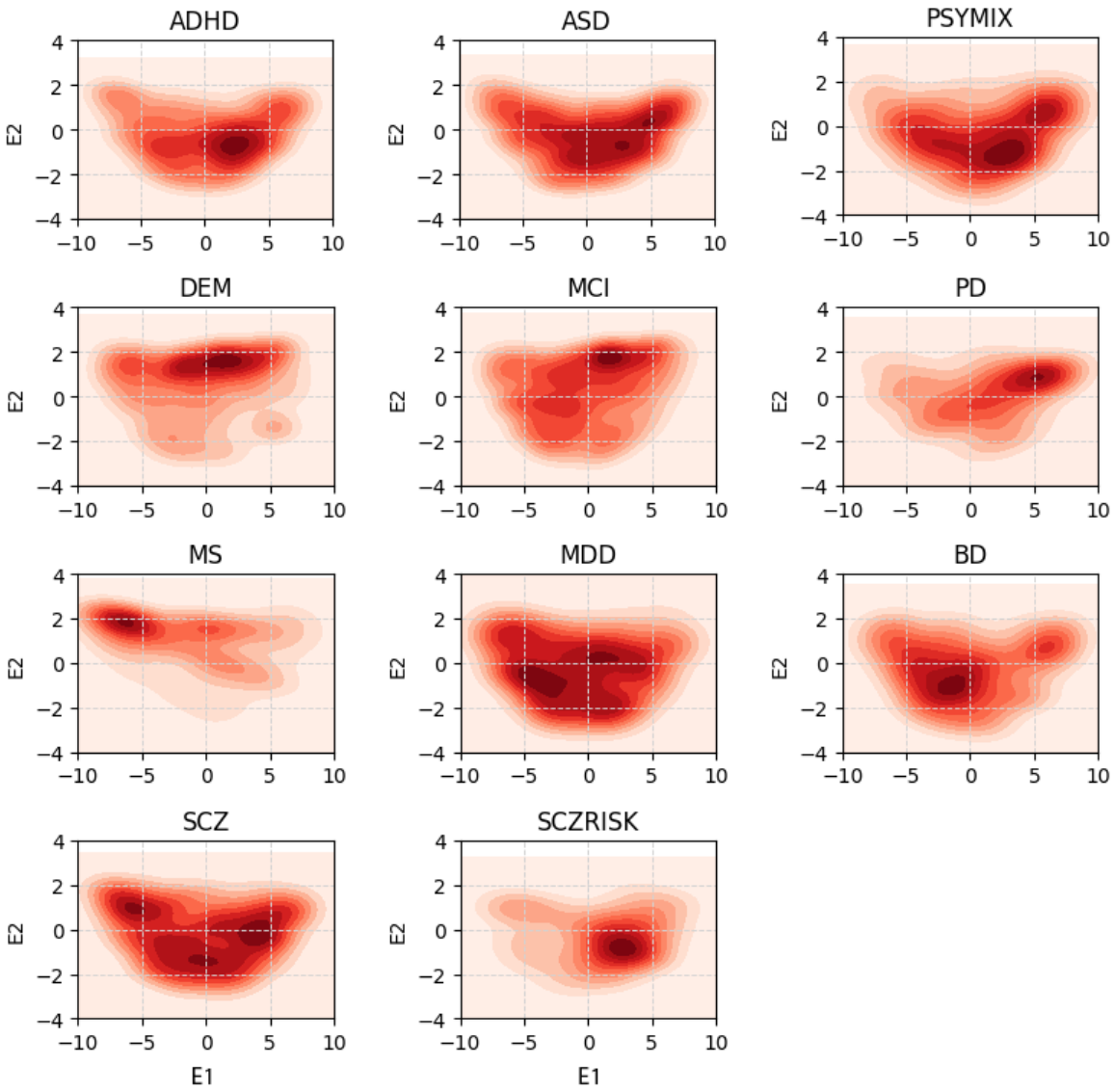

Figure 5. Embedding of all brain disorders in the 2-components space after UMAP dimensionality reduction of the individual thalamic nuclei effects. Colour scale and contours represent the density of occurrences in each area of the 2-D space. Data from each individual for the clinical groups was normalized to the average sample's healthy control group and were submitted to the UMAP algorithm. ADHD: attention deficit and hyperactivity disorder; ASD: autism spectrum disorder; BD: bipolar disorder; DEM: dementia; MCI: mild cognitive impairment; MDD: major depressive disorder; MS: multiple sclerosis; PD: Parkinson's disease; SCZ: schizophrenia; SCZRISK: individuals at clinical high-risk for schizophrenia; PSYMIX: non-SCZ psychosis spectrum diagnoses.